

# Tracking Stem Cells with Magnetic Particle Imaging

## Therapeutic potential of stem cells

Stem cells have the potential to cure numerous degenerative conditions, genetic diseases and physical trauma. As a multipotent progenitor, stem cells can differentiate into important cell lineages both *in vitro* and, in limited situations, after implantation *in vivo*. Over 950 clinical trials are currently underway involving human Mesenchymal Stem Cells (MSCs)<sup>1</sup> for the treatment of diseases such as myocardial infarction, autoimmune diseases, and liver diseases.<sup>2</sup> The applications of stem cells are broad; for example, two recent publications tested MSCs as a treatment for COVID-19-related lung infections.<sup>3,4</sup>

The properties of stem cells extend beyond their multipotent properties. They have been shown to produce many bioactive factors that can improve the functionality of damaged tissue by reducing fibrosis, stimulating neovascularization and endogenous tissue regeneration, as well as providing immunomodulation.<sup>5</sup> In anticancer therapies, MSCs show promise in controlling inflammatory processes by regulating proliferation and cytokine production of immune cells.<sup>6</sup>

The multiple applications to stem cell therapy and current preclinical research to optimize transplantation outcomes require specific and quantitative monitoring methods for the assessment of stem cell implantation following engraftment *in vivo*.

## Stem cell imaging challenges

Noninvasive quantitative monitoring of stem cell delivery and biodistribution is challenging. Optical techniques such as bioluminescence and fluorescence have limited depth penetration and typically use genetically encoded reporters that are complex for clinical translation. Nuclear imaging techniques such as PET or SPECT face limited tracer half-life, significant cumulative radiation dose during

longitudinal studies, and have cost and infrastructure challenges.<sup>7</sup> Magnetic resonance imaging (MRI) with iron oxide nanoparticles has a long history in preclinical and clinical cell tracking. However, T2\* contrast agents in MRI can be difficult to use because of the ambiguity associated with the 'negative' contrast nature of the signal, which complicates image specificity and quantitation.<sup>8</sup>

## Tracking stem cells with Magnetic Particle Imaging

Magnetic Particle Imaging (MPI) is a noninvasive, molecular imaging technique that delivers sensitive, depth-independent images of the spatial distribution of superparamagnetic iron oxide (SPIO) nanoparticle tracers anywhere in an animal. MPI has been demonstrated in multiple preclinical applications, including the tracking of cancer cells, inflammation, tumor-associated macrophages, drug delivery, vascular perfusion, and nanoparticle distribution for localized hyperthermia.<sup>9,10,11,12,13</sup> MPI also scales to human imaging, and clinical scanners are under active development.

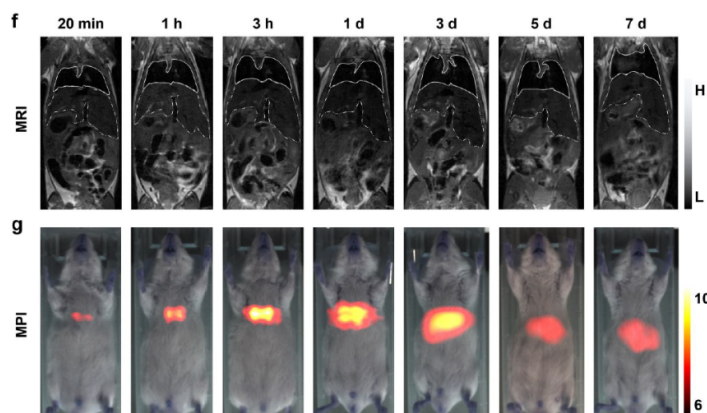


**Figure 1.** MRI & MPI monitoring of labeled MSC biodistribution following i.v. administration. (Top panel) MRI images ( $300 \times 10^3$  MSC/mouse) Lung & liver outlined with white solid lines and dotted lines, respectively. (Bottom panel) Longitudinal 2D projections of MPI signal overlaid on an optical image. ( $100 \times 10^3$  BMSCs). The positive contrast MPI data clearly shows a shift of tracer biodistribution from lungs to liver over 7 days. From reference 17.

MPI is nearly ideal for non-invasive tracking of stem cells. For cell tracking, cells can be labeled with an SPIO tracer prior to implantation. Simple protocols for labelling MSCs with SPIOs are well established and readily available.<sup>14,15,16</sup> After implantation, animals can be longitudinally imaged with MPI. The MPI signal is unambiguous and specific to the SPIO tracers and there is no background from the surrounding tissue. MPI is sensitive with linear signal quantitation, and cells can be imaged quantitatively in deep tissue as the MPI signal does not attenuate with depth. Last, depending on the tracer type, the MPI signal typically remains constant over time, enabling labelled cells to be imaged longitudinally for days to weeks.<sup>17,18</sup>

MPI has a high sensitivity that enables detection of minute tracer quantities. In a single voxel, the MOMENTUM™ imager can routinely detect ~25 ng of the commercially available Synomag® nanoparticle, and has demonstrated detection of 1.1 ng of MPI-optimized particles.<sup>19</sup> Assuming a 2 mm<sup>3</sup> voxel size, this is equivalent to 20-300 picomolar of nanoparticles, or 2.5-56 micromolar Fe. For cells containing 20 picograms of Fe/cell, the detection limit translates to a calculated sensitivity of 50-1250 cells, depending on the tracer. While the limits of sensitivity for cell tracking have yet to be fully tested, multiple groups have demonstrated *in vivo* cell detection in the ~250 cell range.<sup>18,20</sup>

## MPI of bone marrow-derived stem cells

Bone marrow-derived stem cells (BMSCs) are a subset of MSCs important for growth and repair of skeletal tissues such as cartilage and bone. BMSCs may provide an unlimited source of tissue with potentially better engraftment<sup>21</sup> success than conventional bone transplant therapies, which have a low success rate due to hostile environment and rejection. As researchers work to improve BMSC transplants, there is a need for non-invasive methods to quantitatively measure the success of grafts and validate stem cell-based regeneration approaches.<sup>2,14</sup>

Figure 1 (previous page) demonstrates how MPI can track the biodistribution of SPIO-labeled BMSCs following intravenous delivery. In the image, we see longitudinal, side-by-side MRI and MPI monitoring of SPIO labeled BMSCs. MPI and MRI provide complementary images, with MPI filling in the T2\* signal voids in the MRI. Further, MPI imaging shows how the tracer in the BMSCs redistribute from the lungs to the liver over time, a change not readily visible in the MRI images.<sup>17</sup>

Figure 2 shows how MPI can monitor homing of BMSCs during femur ischemia. Control and ischemic mice received intramuscular injections of SPIO-labeled BMSCs in the gastrocnemius muscle.

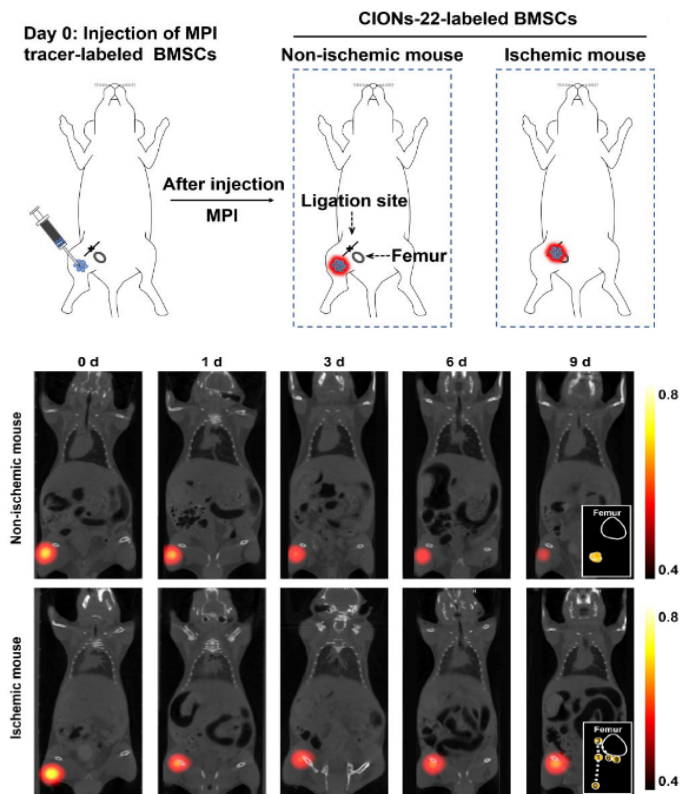


**Figure 2.** MPI-CT imaging of SPION-labeled BMSCs after intramuscular injection. (Top) Schematic illustration of the biodistribution pattern of BMSCs in ischemic vs non-ischemic mice following injection. (Middle, bottom) MPI-CT signal CION-22-labeled BMSCs in non-ischemic (middle) or ischemic (bottom) mice over 9 days. The inset is the illustrative trajectory of transplanted stem cells, with numbers indicating the location at different days. Taken from reference 17.

Animals were imaged longitudinally for 9 days with MPI and X-ray/CT. BMSCs migration toward the ligation site are observed by MPI, consistent with previous reports that stem cells can migrate to damaged tissue in response to inflammatory factors.<sup>22</sup>

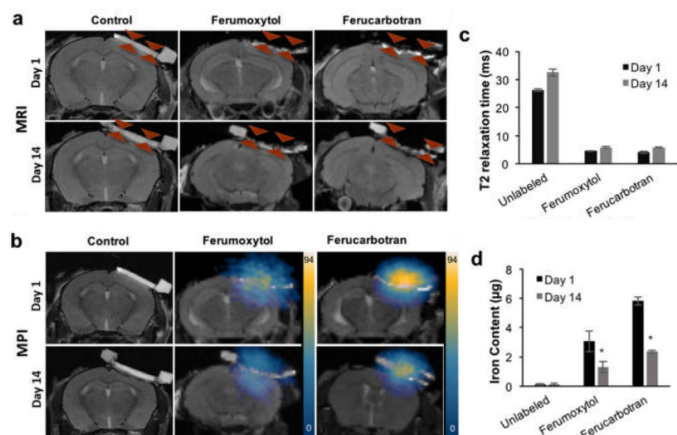


Fig. 3. In vivo MRI and MPI of labeled MSC implants in calvarial defects day 1 and 14 post implantation of unlabeled, ferumoxytol or ferucarbotran-labeled stem cells. (a). Coronal fast spin echo MRI image (FSE; TE/TR = 42 ms/3000 ms). (b). Corresponding MPI images of the same calvarial defects. (c). Corresponding T2 relaxation times. (d). Co-registered Fe quantification estimated from the MPI signals of the MSC implants. Data are displayed as means and standard deviations of three animals per experimental group. Taken from reference 23.

Shown in Figure 3, Nejadnik et al.<sup>23</sup> use a MPI system to monitor a BMSC treatment of a murine calvarial bone defect model. The study monitored ferucarbotran-labeled BMSCs implanted in PEG-dimethacrylate scaffolds over 14 days and compared T2\* MRI with MPI. The MPI data quantitated stem cell survival, which was not possible with T2\* MRI. Co-registering the MPI and MRI images enabled both localization and quantification of the stem cell implantation.

An experiment worthy of mention is a trimodal study combining MPI with iron- and fluorine-based MRI (not shown here). The study used MPI to monitor implantation of ferumoxytol-labeled MSCs in the hindlimb muscle of C57Bl/6 mice, fluorine MRI to monitor the ensuing inflammation, and proton MRI for anatomic localization.<sup>24</sup>

## MPI of neural progenitor cells

In Figure 4, we see how MPI can be used for quantitative and high sensitivity monitoring of neural stem cell grafts. First, human embryonic stem cells were differentiated into neural progenitor cells and labeled. Following implantation in a rat brain, the grafts were monitored by MPI over 87 days. The authors also demonstrated that the MPI signal was linear with increasing nanoparticle concentration.<sup>18</sup> They concluded that MPI has a strong potential for monitoring neural stem cell transplants.

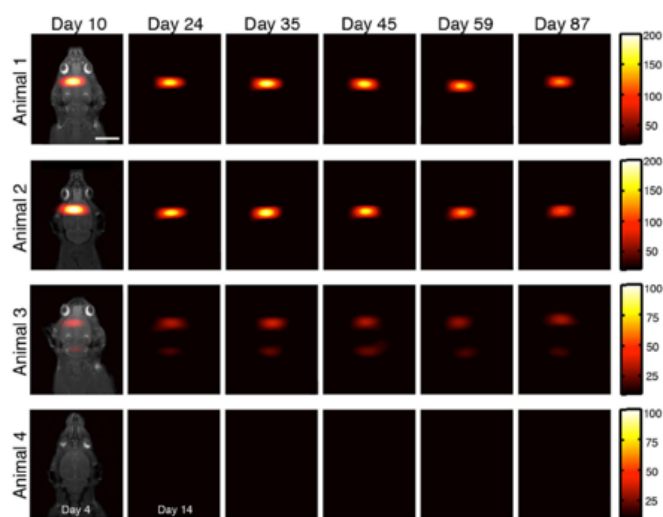


Figure 4. MPI quantitatively tracks NPC neural implants in rats over 87 days. Longitudinal MPI imaging of SPIO-labeled human NPCs implanted in the forebrain cortex (Animals 1-2), near lateral ventricle (Animal 3), and equivalent SPIO-only tracer in the forebrain cortex as control (Animal 4). MPI imaging quantifies graft clearance and movement over time, with rapid total clearance of SPIO-only. From reference 18.

## MOMENTUM™ and stem cell tracking

Magnetic Insight's MOMENTUM™ MPI system is the world's first self-shielded preclinical MPI solution. Using a strong field-free-line gradient and a proprietary X-space reconstruction process, the MOMENTUM™ produces high resolution MPI images with high sensitivity. With an extensive track record of publications, MPI is ideal for longitudinal monitoring and quantification of stem cells *in vivo*.<sup>17,18,23,24</sup> The MOMENTUM™ is also available with an integrated CT option for easy anatomical co-registration.

## Conclusions

As stem cell research moves from cell culture work to preclinical and clinical studies, researchers increasingly require *in vivo* imaging tools. These tools must enable accurate localization and precise quantitation of cell graft implantation, especially in longitudinal studies. MPI offers researchers a complementary solution to traditional medical imaging technology and fills the voids inherent to MRI, PET, SPECT and optical imaging.

*Synomag® is a registered trademark of micromod Partikeltechnologie GmbH, Germany.*

## References

1. Pittenger et al, npj Regenerative Medicine (2019) 4, 22. DOI: 10.1038/s41536-019-0083-6
2. Zakrzewski et al. Stem Cell Research & Therapy (2019) 10, 68. DOI:10.1186/s13287-019-1165-5
3. Z. Leng et al., "Transplantation of ACE2-mesenchymal stem cells improves the outcome of patients with COVID-19 pneumonia," Aging and Disease, 11:216–28, 2020. DOI: 10.14336/AD.2020.0228
4. B. Liang et al., "Clinical remission of a critically ill COVID-19 patient treated by human umbilical cord mesenchymal stem cells," ChinaXiv, 202002.00084, 2020.
5. Butler, J. et al. Circ. Res. (2017) 120, 332–340. DOI: 10.1161/CIRCRESAHA.116.309717
6. Lin et al. BioMed Research International (2019) Article ID 2820853, DOI: 10.1155/2019/2820853
7. Nguyen et al. Cell Stem Cell (2014) 14, 431–44. DOI: 10.1016/j.stem.2014.03.009
8. Wang & Shan. J Basic Clin Med. (2012) 1, 1–6. PMID: 24159426.
9. Wu et al. Am. J. Neuroradiol. (2019) 40, 2, 206–212. DOI: 10.3174/ajnr.A5896
10. Makela et al. Molecular Imaging in Biology (2020). DOI: 1007/s11307-020-01473-0
11. Zhu et al. Nano Lett. (2019) 19, 6725–6733. DOI: 10.1021/acs.nanolett.9b01202
12. Song et al. Nat Biomed Eng (2020) 4, 325–334. DOI: 10.1038/s41551-019-0506-0
13. Tay et al. ACS Nano (2018) 12, 4, 3699–3713. DOI: 2018, 12, 4, 3699–3713
14. Zheng et al. Theranostics (2016) 6, 291–301. DOI: 10.7150/thno.13728
15. Noorwali et al. Bioinformation (2019) 15, 1–10. DOI: 10.6026/97320630015001
16. Lin et al. Nanomaterials (2017) 7, 107. DOI: 10.3390/nano7050107
17. Wang et al. ACS Nano (2020) 14, 2, 2053–2062. DOI: 10.1021/acsnano.9b08660
18. Zheng et al. Scientific reports (2015) 5, 14055. DOI: 10.1038/srep14055
19. H. Arami, E. Teeman, A. Troska, H. Bradshaw, K. Saatchi, A. Tomitaka, S. Gambhir, U. O. Hafeli, D. Liggitt and K. Krishnan, Nanoscale, 2017, DOI: 10.1039/C7NR05502A.
20. Song, et al Nano Lett. (2018) 10, 182–189. DOI: 10.1021/acs.nanolett.7b03829, 13, 7, 7750–7758
21. Chimutengwende-Gordon & Khan. Curr. Stem. Cell. Res. Ther. (2012) 7, 122–126. DOI: 10.2174/157488812799219036
22. Uccelli et al. Nat.Rev. Immunol. (2008) 8, 726–736. DOI: 10.1038/nri2395.
23. Nejadnik et al. Mol Imaging Biol (2019) 21, 465–472. DOI: 10.1007/s11307-018-1276-x
24. Sehl et al. Tomography (2019) DOI: 10.18383/j.tom.2019.00020